Int. J. Solids Structures Vol. 23, No. 9, pp. 1247–1268, 1987
Printed in Great Britain.

0020-7683/87 $3.00 + .00

THE EFFECT OF MICRO-CRACK SYSTEMS ON THE LOSS OF STIFFNESS OF BRITTLE SOLIDS

N. LAWS
Department of Mechanical Engineering, University of Pittsburgh, Pittsburgh, PA 15261, U.S.A.

and

J. R. BROCKENBROUGH
Alcoa Laboratories, Alcoa Center, PA 15069, U.S.A.

(*Received* 26 *May* 1986; *in revised form* 29 *December* 1986)

Abstract—Micro-cracks in a fabricated ceramic reduce stiffness compared with the ideal ceramic. Self-consistent estimates for stiffness reduction are obtained for a variety of crack shapes and orientation distributions. Results are derived in terms of a common measure of crack density which allows different crack systems to be compared. In particular we consider cracking along grain boundaries of a two-dimensional hexagonal array which leads to overall anisotropy of the ceramic. It is found that knowledge of crack number density, orientation distribution, and crack geometry are all needed in order to predict loss of stiffness. Closed form solutions are derived which are entirely adequate for most engineering applications.

1. INTRODUCTION

This paper is devoted to the study of the effect of micro-cracks on the elastic response of brittle solids. It is well known, see for example Case[1] and the references contained therein, that the elastic moduli can be significantly affected by micro-cracks. Accordingly, a major aim of this paper is to discuss the effect of micro-crack geometry and density on the loss of stiffness of brittle solids. It need hardly be emphasized that knowledge of the loss of stiffness is a prerequisite for any calculations of micro-crack toughening, etc.

The fundamental paper for most of the recent work on cracked brittle solids, in both materials science and geophysics, is due to Budiansky and O'Connell[2]. Indeed the self-consistent analysis provided by these authors provides the starting point for most analyses of micro-cracking in ceramics, see e.g. Refs [3–7]. As far as we are aware all work, thus far, on the application of the theory to micro-cracked brittle solids assumes that micro-cracks are penny-shaped and randomly oriented. However, as is discussed by Budiansky and O'Connell[2] this assumption, while convenient, is not essential. In fact the analysis in Ref. [2] applies to randomly oriented ellipsoids. From the point of view of applications, perhaps the most obvious disadvantage of the Budiansky and O'Connell[2] analysis is that it is restricted to randomly oriented micro-cracks and hence to solids which in the cracked state are isotropic. This situation was quickly recognized and various authors, with diverse applications in mind, addressed the problem of formulating a self-consistent analysis for anisotropic distributions of cracks, see Refs [8–12]. It is perhaps important to emphasize that the work of Hoenig[8], Gottesman *et al.*[9], Laws *et al.*[10], and Laws and Dvorak[12] assumes that the cracks are *open*. An exception is the paper by Horii and Nemat-Nasser[11] which specifically addresses the problem of closed and open cracks. We emphasize that the considerations of this paper are restricted to *open cracks*.

In connection with the work on ceramics by Evans[3], Evans and Faber[4], and Fu and Evans[5–7], it is clear that use of a *model* which assumes a random distribution of penny-shaped cracks is useful. However, we can construct other models which are, in certain circumstances, more physically appealing and thus, perhaps, more useful. In particular, following the suggestion of Fu and Evans[6], one can construct a model of a close packed hexagonal aggregate with cracks on the respective interfaces.

Clearly a major problem is that, at the present time, we can only hypothesize potential micro-crack geometries. It is, therefore, imperative to construct a general model so that one

can analyze the effects of various crack geometries. Hence, a major part of this paper consists of a general analysis of the loss of stiffness of elastic solids containing various families of micro-cracks. More precisely the contents of the paper are as follows. In Section 2 we collect some known results on cracks in anisotropic solids. For the purposes of our later development the crucial quantity is the energy released by the introduction of a single crack in an infinite solid. We give the required results for elliptical cracks, penny-shaped cracks and slit cracks. Section 3 contains a new and completely general derivation of the self-consistent model for distributions of elliptical and slit cracks in anisotropic solids. This analysis simplifies and extends the results which are currently available. The derivation is obtained from a variant of a standard argument in fracture mechanics—and is, in fact, a generalization of some analysis given by Budiansky and O'Connell[2]. For technical reasons it is essential to consider elliptical cracks separately from slit cracks.

Special cases which are particularly relevant in the study of brittle solids are considered in later sections. In order to be able to compare cracks with different plan forms we make use of the crack density parameter introduced by Budiansky and O'Connell[2]. It is not clear to the present authors that the chosen parameter is the most convenient, or physically attractive, choice. At least it has the merit that it enables us to compare widely different crack systems—albeit with considerable difficulty. Two geometries which are chosen for special study are randomly oriented elliptical cracks and randomly oriented slit cracks. Following Budiansky and O'Connell[2] we investigate the feasibility of replacing elliptical cracks by penny-shaped cracks. With proper interpretation, the replacement is acceptable. We go on to discuss aligned slit cracks and penny-shaped cracks and here show how to recover some results of Hoenig[8], Laws *et al.*[10], and Laws and Dvorak[12].

Next, we investigate the stiffness loss due to two distributions of two-dimensionally oriented slit cracks. This work has no parallel in the literature and would appear to have some importance in the study of polycrystalline aggregates. In the first place we consider a family of slit cracks whose normals are randomly oriented in a fixed plane, see also Horii and Nemat-Nasser[11]. Second, we consider a hexagonal close packed array with cracks on various facets as suggested by Fu and Evans[6]. It is noteworthy that both models give rise to the same stiffness reduction.

Numerical results for the various cases are given in the respective sections. But Section 9 contains some comparisons between different crack systems. It is not easy to summarize the results. However, it is appropriate to mention that in most current problems in materials science known to the authors, the *dilute* results should be entirely adequate. From a practical point of view the significance of this observation is that one can use *explicit* formulae for the loss in stiffness rather than have to resort to numerical methods. Finally, we emphasize that the results obtained herein indicate that the loss of stiffness of a brittle solid depends upon both the micro-crack geometry and the density of micro-cracks. As is shown in Section 9, for given density of micro-cracks, differences in geometry can produce dramatic differences in effective elastic moduli.

2. PRELIMINARIES

We follow a standard practice in the theory of composite materials and use the notation introduced by Hill[13]. Fourth-order tensors are denoted by upper case letters, e.g. M, Λ; symmetric second-order tensors are denoted by lower case Greek letters, e.g. $\boldsymbol{\sigma}$, $\boldsymbol{\varepsilon}$, and vectors are denoted by lower case Roman letters, e.g. $\mathbf{t}$, $\mathbf{u}$. A dot denotes the appropriate inner product.

Consider an anisotropic linear elastic solid whose stiffness is L and whose compliance is M. Thus, the stress, $\boldsymbol{\sigma}$, and strain, $\boldsymbol{\varepsilon}$, are related through

$$\boldsymbol{\sigma} = L\boldsymbol{\varepsilon}, \qquad \boldsymbol{\varepsilon} = M\boldsymbol{\sigma}. \tag{1}$$

In this paper, the theoretical development is more easily understood when we make exclusive use of the compliance M. The most general form of anisotropy which is relevant to our present discussion is orthotropy with respect to the three coordinates planes $0x_1x_2x_3$. In

such circumstances, it is best to use standard 6×6 engineering notation, so that $\varepsilon_1 = \varepsilon_{11}$, $\varepsilon_6 = 2\varepsilon_{23}$, etc. For orthotropy, eqns (1) may be written in the component form

$$\begin{bmatrix} \varepsilon_1 \\ \varepsilon_2 \\ \varepsilon_3 \\ \varepsilon_4 \\ \varepsilon_5 \\ \varepsilon_6 \end{bmatrix} = \begin{bmatrix} M_{11} & M_{12} & M_{13} & 0 & 0 & 0 \\ & M_{22} & M_{23} & 0 & 0 & 0 \\ & & M_{33} & 0 & 0 & 0 \\ & & & M_{44} & 0 & 0 \\ & \text{SYM} & & & M_{55} & 0 \\ & & & & & M_{66} \end{bmatrix} \begin{bmatrix} \sigma_1 \\ \sigma_2 \\ \sigma_3 \\ \sigma_4 \\ \sigma_5 \\ \sigma_6 \end{bmatrix} \tag{2}$$

or, in terms of Young's moduli and Poisson's ratios

$$\begin{bmatrix} \varepsilon_1 \\ \varepsilon_2 \\ \varepsilon_3 \\ \varepsilon_4 \\ \varepsilon_5 \\ \varepsilon_6 \end{bmatrix} = \begin{bmatrix} 1/E_{11} & -\nu_{12}/E_{11} & -\nu_{13}/E_{11} & 0 & 0 & 0 \\ & 1/E_{22} & -\nu_{23}/E_{22} & 0 & 0 & 0 \\ & & 1/E_{33} & 0 & 0 & 0 \\ & & & M_{44} & 0 & 0 \\ & \text{SYM} & & & M_{55} & 0 \\ & & & & & M_{66} \end{bmatrix} \begin{bmatrix} \sigma_1 \\ \sigma_2 \\ \sigma_3 \\ \sigma_4 \\ \sigma_5 \\ \sigma_6 \end{bmatrix}. \tag{3}$$

Of course, M_{44}, M_{55} and M_{66} are merely the reciprocals of the respective shear moduli.

We are also particularly concerned with transversely isotropic materials. When $0x_3$ is the axis of transverse isotropy

$$M_{11} = M_{22}, \quad M_{13} = M_{23}, \quad M_{44} = M_{55}, \quad M_{66} = 2(M_{11} - M_{12}). \tag{4}$$

There are corresponding relations between the Young's moduli, Poisson's ratios and transverse shear moduli.

At this point it is advantageous to consider several crack problems.

2.1. *Slit cracks*

First consider a slit crack defined by

$$-a \leqslant x_1 \leqslant a, \qquad x_2 = 0, \qquad |x_3| < \infty \tag{5}$$

in an orthotropic elastic solid. The loading of the solid at infinity is prescribed such that it is compatible with a crack-opening uniform stress $\boldsymbol{\sigma}^{\mathrm{A}}$. This problem has received considerable attention and its solution is well known; see e.g. Stroh[14], Lekhnitskii[15], Sih *et al.*[16]. Of major concern in the sequel is the interaction energy due to the crack, or, what is equivalent, the total energy released by the introduction of the crack under fixed loading $\boldsymbol{\sigma}^{\mathrm{A}}$. It is not difficult to show that the energy released per unit length by introduction of the slit crack is, see Laws[17]

$$\mathscr{E} = \tfrac{1}{2}\pi a^2 \boldsymbol{\sigma}^{\mathrm{A}} \cdot \boldsymbol{\Lambda}^{\mathrm{S}} \boldsymbol{\sigma}^{\mathrm{A}}. \tag{6}$$

The superscript S indicates that this is the $\boldsymbol{\Lambda}$ tensor for slits. The only non-zero components of $\boldsymbol{\Lambda}^{\mathrm{S}}$ are given by

$$\begin{aligned} \Lambda^{\mathrm{S}}_{22} &= \frac{M_{22}M_{33} - M_{23}^2}{M_{33}} (\alpha_1^{1/2} + \alpha_2^{1/2}), \\ \Lambda^{\mathrm{S}}_{44} &= (M_{44}M_{55})^{1/2}, \\ \Lambda^{\mathrm{S}}_{66} &= \frac{(M_{22}M_{33} - M_{23}^2)^{1/2}(M_{11}M_{33} - M_{13}^2)^{1/2}}{M_{33}} (\alpha_1^{1/2} + \alpha_2^{1/2}) \end{aligned} \tag{7}$$

where α_1 and α_2 are the roots of

$$(M_{22}M_{33}-M_{23}^2)\alpha^2-[M_{33}M_{66}+2(M_{12}M_{33}-M_{13}M_{23})]\alpha+M_{11}M_{33}-M_{13}^2=0. \quad (8)$$

Obviously the non-zero components of Λ^S which are listed above only depend upon the compliances of the solid. This property is needed later.

2.2. *Elliptical cracks*

Consider next an elliptical crack defined by

$$\frac{x_1^2}{a^2}+\frac{x_2^2}{b^2}\leqslant 1, \qquad x_3=0 \quad (9)$$

in an infinite solid. When the solid is orthotropic it is not possible, in general, to give an analytical solution. Rather, one must resort to numerical methods to compute the interaction energy, see Hoenig[8]. Fortunately our present problems are adequately handled by considering an elliptical crack in an isotropic material, and a penny-shaped crack in a transversely isotropic material.

First, consider the elliptical crack, defined by expressions (9), in an isotropic material. Then it follows from the results of Budiansky and O'Connell[2] that the interaction energy, $\mathscr{E}$, is given by

$$\mathscr{E}=\tfrac{2}{3}\pi ab^2\boldsymbol{\sigma}^A\cdot\Lambda^c\boldsymbol{\sigma}^A \quad (10)$$

where the non-zero components of Λ^c are given by

$$\Lambda^c_{33}=\frac{2(1-\nu^2)}{E}\frac{1}{E(k)}, \qquad \Lambda^c_{44}=\frac{2(1-\nu^2)}{E}Q(k,\nu), \qquad \Lambda^c_{55}=\frac{2(1-\nu^2)}{E}R(k,\nu). \quad (11)$$

Here $E(k)$ is the complete elliptic integral of the second kind with argument $k=(1-b^2/a^2)^{1/2}$. Also

$$R(k,\nu)=k^2\{(k^2-\nu)E(k)+\nu(1-k^2)K(k)\}^{-1}$$
$$Q(k,\nu)=k^2\{[k^2+(1-k^2)]E(k)-\nu(1-k^2)K(k)\}^{-1}$$

where $K(k)$ is the complete elliptic integral of the first kind.

We note that the non-zero components of Λ^c listed in eqns (11) depend only upon the aspect ratio b/a of the ellipse. This observation has important consequences in our discussion of cracked solids.

2.3. *Penny-shaped crack*

Next consider a penny-shaped crack

$$x_1^2+x_2^2\leqslant a^2, \qquad x_3=0$$

in a solid transversely isotropic with respect to $0x_3$. This problem has been studied by Shield[18], Chen[19], Mura[20], Laws[21] and others. The interaction energy is given by Laws[21] in the form

$$\mathscr{E} = \tfrac{2}{3}\pi a^3 \sigma^{\Lambda} \cdot \Lambda^{P} \sigma^{\Lambda} \tag{12}$$

where the non-zero components of Λ^P are given by

$$\begin{aligned} \Lambda^P_{33} &= \frac{2\gamma_1\gamma_2(\gamma_1+\gamma_2)}{\pi}\frac{M_{11}^2 - M_{12}^2}{M_{11}}, \\ \Lambda^P_{44} = \Lambda^P_{55} &= \frac{4(\gamma_1+\gamma_2)(M_{11}^2 - M_{12}^2)(2M_{44})^{1/2}}{\pi[M_{11}(2M_{44})^{1/2} + (\gamma_1+\gamma_2)(M_{11}+M_{12})(M_{11}-M_{12})^{1/2}]} \end{aligned} \tag{13}$$

and γ_1^2, γ_2^2 are the roots of

$$(M_{11}^2 - M_{12}^2)x^2 - [M_{11}M_{44} + 2M_{13}(M_{11} - M_{12})]x + M_{11}M_{33} - M_{13}^2 = 0. \tag{14}$$

We note that the non-zero components of Λ^P are independent of the crack radius a.

In the next section we use the preceding expressions for the interaction energy to obtain the self-consistent estimates of the effective compliances of a solid containing micro-cracks. Obviously, for a penny-shaped crack in an isotropic material Λ^e given by eqns (10) and (11) and Λ^P given by eqns (12)–(14) reduce to a common form to give the standard result, see e.g. Eshelby[22].

3. THE SELF-CONSISTENT MODEL

The use of the self-consistent model in the study of cracked solids is now extensive. The pioneering work by Budiansky and O'Connell[2] has been elaborated and extended by Hoenig[8], Gottesman *et al.*[9], Laws *et al.*[10], Horii and Nemat-Nasser[11] and others. The aim here is to give a concise, completely general derivation of the self-consistent model which is apparently not to be found in the literature. Obviously our derivation can be specialized to give the results of the above-mentioned authors. Such results that are necessary for our purpose will be given in the text.

From the point of view of the study of micro-cracking, it is essential to develop the theory once and for all. Indeed, since the precise geometry of the micro-crack systems is often unknown, an important role of the model will be to permit the study of the influence of various micro-crack geometries on the loss of stiffness. A compact, yet fully general, derivation of the self-consistent model is furnished by a modification of some standard arguments in linear elastic fracture mechanics. Thus consider an uncracked solid with volume V. Next consider the same solid which now contains a family of similar cracks. We only consider families of cracks whose plan form is either elliptical or rectangular. An essential feature of the contemplated geometries is that each crack has similar geometry. Thus when we consider a family of ellipses, these ellipses *must* have fixed aspect ratio b/a. The same must be true for families of slit cracks. While we only consider a single family of cracks in any one solid, the generalization to allow for several families of cracks is trivial.

In our study of solids containing micro-cracks, it is essential to consider V to be subject to macroscopically uniform loading, see Hill[13]. For our present purposes it suffices to consider loading on the outer surface, S, which is compatible with *uniform* stress $\bar{\sigma}$. The total potential energy of the uncracked elastic solid within V is

$$E_0 = \int_V \tfrac{1}{2}\boldsymbol{\sigma}\cdot\boldsymbol{\varepsilon}\, dV - \int_S \mathbf{t}\cdot\mathbf{u}\, dS \tag{15}$$

$$= -\tfrac{1}{2}V\bar{\sigma}\cdot M_0\bar{\sigma} \tag{16}$$

where M_0 is the compliance tensor of the *uncracked* solid. Likewise, we can show that the total energy of the cracked solid is

$$E = -\tfrac{1}{2}V\bar{\sigma}\cdot M\bar{\sigma} \tag{17}$$

where M is the effective compliance tensor of the *cracked* solid. A standard concept in fracture mechanics indicates that

$$\mathscr{E}_{\text{tot}} = \text{energy released by the system of cracks} = E_0 - E. \tag{18}$$

Up to this point the analysis is exact.

We now use the self-consistent model to *estimate* the energy released by the system of cracks. This estimate is dependent on the specific geometry of a typical crack.

3.1. *Slit cracks*

First, let us suppose that the solid contains a distribution of similar slit cracks of width $2a$ and length l but with constant aspect ratio $l/2a \gg 1$. The essential step in the self-consistent method is to estimate the energy released by a typical crack by calculating the energy released by this *single* crack in an infinite solid having the effective properties of the cracked solid. Now for a *typical slit crack* we see from eqn (6) that

$$\mathscr{E} = \tfrac{1}{2}\pi a^2 l\bar{\sigma}\cdot\Lambda^{\text{S}}\bar{\sigma} \tag{19}$$

where the components of Λ^{S} can be obtained from eqns (7). In view of the self-consistent methodology, the compliances occurring in eqns (7) and (8) are those of the *cracked* solid. Since the micro-crack systems of interest usually involve oriented cracks it is clear that the total energy released by the system of slit cracks is given by

$$\mathscr{E}_{\text{tot}} = NV\{\mathscr{E}\} \tag{20}$$

where N is the number of cracks per unit volume and $\{\ \}$ denotes the average of the bracketed quantity. Now Λ^{S} is independent of the aspect ratio l/a, so provided crack size and orientation are not correlated, it follows that

$$\{\mathscr{E}\} = \tfrac{1}{2}\pi\{a^2 l\}\bar{\sigma}\cdot\{\Lambda^{\text{S}}\}\bar{\sigma}. \tag{21}$$

In eqn (21), $\{a^2 l\}$ denotes the gross average of $a^2 l$, whereas $\{\Lambda^{\text{S}}\}$ denotes the orientation average of $\{\Lambda^{\text{S}}\}$. A natural choice for the dimensionless crack density parameter is suggested by eqn (21), namely

$$\beta = N\{a^2 l\}. \tag{22}$$

With the help of eqns (16)–(22) it now follows that

$$\frac{\pi}{2}\beta\bar{\sigma}\cdot\{\Lambda^{\text{S}}\}\bar{\sigma} = -\tfrac{1}{2}\bar{\sigma}\cdot M_0\bar{\sigma} + \tfrac{1}{2}\bar{\sigma}\cdot M\bar{\sigma}.$$

But M, M_0 and $\{\Lambda^{\text{S}}\}$ are symmetric and $\bar{\sigma}$ is arbitrary; hence

$$M = M_0 + \pi\beta\{\Lambda^{\text{S}}\}. \tag{23}$$

For a given orientation distribution, eqn (23) provides the self-consistent equation for the determination of the effective compliances of the cracked solid.

3.2. *Elliptical cracks*

Next suppose that our solid contains a distribution of elliptical cracks. For arbitrary anisotropy the interaction energy is given by eqn (10); however, as emphasized earlier, analytic forms for the components of Λ^{e} can only be found in special cases. For the time

being we can proceed in full generality. Indeed a minor variant of the argument that starts at eqn (18) and ends at eqn (21) shows that the self-consistent estimates for a solid containing variously oriented elliptical cracks of constant aspect ratio b/a are to be obtained from

$$M = M_0 + \tfrac{4}{3}\pi\alpha\{\Lambda^e\} \tag{24}$$

where the crack density parameter α is here defined by

$$\alpha = N\{ab^2\}. \tag{25}$$

It is useful to note that Budiansky and O'Connell[2] use a different crack density parameter

$$\varepsilon = \frac{\pi\alpha}{2E(k)} = \frac{2N}{\pi}\left\{\frac{A^2}{P}\right\} \tag{26}$$

where A is the area of a crack and P its perimeter. As is discussed later it is better to use ε, rather than α, as the crack density parameter.

Now suppose that our solid contains a distribution of penny-shaped cracks. It is easy to show that the self-consistent estimates for the effective compliances of a solid containing variously oriented penny-shaped cracks are to be obtained from

$$M = M_0 + \tfrac{4}{3}\pi\varepsilon\{\Lambda^p\} \tag{27}$$

where the crack density parameter ε is given by

$$\varepsilon = N\{a^3\}. \tag{28}$$

4. RANDOMLY ORIENTED ELLIPTICAL CRACKS

In this section we consider a solid which contains a distribution of elliptical cracks. Thus the governing equation of the self-consistent model is eqn (24)

$$M = M_0 + \tfrac{4}{3}\pi\alpha\{\Lambda^e\}. \tag{29}$$

For randomly oriented ellipses in a solid which is *isotropic* in its uncracked state, the work of Budiansky and O'Connell[2] is paramount. While we do not propose to rederive a significant part of the Budiansky and O'Connell[2] analysis, it is, perhaps, of interest to show how to derive their equations from the *general* model given in eqn (29). Thus, we first note that the non-zero components of Λ^e for a crack normal to the x_3-axis are given in eqns (11). Obviously, the components of Λ^e for cracks with alternative orientation can be found by a simple change of coordinates. However, for a completely (three-dimensionally) random orientation distribution of cracks, such coordinate changes are not necessary. Rather, we can use a technique due to Kröner[23] which enables us to compute the orientation average of Λ^e once the components of Λ^e for a single orientation are known. In terms of standard Cartesian tensor notation, Kröner's[23] result may be given as follows. Let Λ^e_{ijkl} be the Cartesian tensor components of Λ^e. Since all orientations of cracks are equally likely the orientation average $\{\Lambda\}$ will be isotropic. Hence

$$\{\Lambda^e\}_{ijkl} = \eta(\delta_{ik}\delta_{jl} + \delta_{il}\delta_{jk} - \tfrac{2}{3}\delta_{ij}\delta_{kl}) + \xi\delta_{ij}\delta_{kl}. \tag{30}$$

It then follows that

$$9\xi = \Lambda^e_{iikk} \tag{31}$$

$$3\xi + 10\eta = \Lambda^e_{ijij} \tag{32}$$

where we can compute the right-hand sides of eqns (31) and (32) from the components of Λ^c in any coordinate system since they are invariants. It now remains for us to translate Kröner's[23] result into standard 6×6 notation. First we note that

$$\Lambda_{33} = \Lambda_{3333}, \qquad \Lambda_{44} = 4\Lambda_{2323}, \qquad \Lambda_{55} = 4\Lambda_{3131}, \quad \text{etc.}$$

Thus

$$\{\Lambda^c\}_{11} = \{\Lambda^c\}_{22} = \{\Lambda^c\}_{33} = \xi + \tfrac{4}{3}\eta = \tfrac{1}{3}\Lambda^c_{33} + \tfrac{1}{15}(\Lambda^c_{44} + \Lambda^c_{55}) \tag{33}$$

$$\{\Lambda^c\}_{12} = \{\Lambda^c\}_{13} = \{\Lambda^c\}_{23} = \xi - \tfrac{2}{3}\eta = \tfrac{1}{15}\Lambda^c_{33} - \tfrac{1}{30}(\Lambda^c_{44} + \Lambda^c_{55}) \tag{34}$$

$$\{\Lambda^c\}_{44} = \{\Lambda^c\}_{55} = \{\Lambda^c\}_{66} = 4\eta = \tfrac{4}{15}\Lambda^c_{33} + \tfrac{1}{5}(\Lambda^c_{44} + \Lambda^c_{55}). \tag{35}$$

The Budiansky and O'Connell[2] equations may now be obtained from the component form of eqn (29), together with eqns (4), (11) and (33)–(35). In particular it is easy to show that the diagonal components yield

$$\frac{E}{E_0} = 1 - \varepsilon\frac{16(1-\nu^2)}{45}[3 + (Q+R)E(k)] \tag{36}$$

$$\frac{G}{G_0} = 1 - \varepsilon\frac{8(1-\nu)}{45}[4 + 3(Q+R)E(k)] \tag{37}$$

which coincide with the results of eqns (39) and (44) of Budiansky and O'Connell[2]. We remark that further algebraic manipulation recovers all of the results given in Ref. [2] for dry elliptical cracks.

For completeness, we give below the reduced form of eqns (36) and (37) for penny-shaped cracks. In this case we have

$$Q(k, \nu) = \frac{4}{\pi(2-\nu)}, \qquad R(k, \nu) = \frac{4}{\pi(2-\nu)}, \qquad E(k) = \pi/2$$

so that

$$\frac{E}{E_0} = 1 - \varepsilon\frac{16(1-\nu^2)(10-3\nu)}{45(2-\nu)} \tag{38}$$

$$\frac{G}{G_0} = 1 - \varepsilon\frac{32(1-\nu)(5-\nu)}{45(2-\nu)} \tag{39}$$

as first shown by Budiansky and O'Connell[2]. Since we can express ν in terms of E and G, it is a simple matter to solve eqns (36) and (37) for E, G, ν, etc. Numerical solutions for the various elastic moduli have been given in Fig. 5 of Budiansky and O'Connell[2].

A significant conclusion which is drawn by these authors is that the stiffness loss predicted by eqns (36) and (37) is insensitive to the aspect ratio of the ellipses and depends only on ε. This observation prompts the study of families of randomly oriented penny-shaped cracks which is prevalent in the analysis of micro-cracked ceramics, see Refs [5–7]. For a given aspect ratio (of the family of ellipses) it is necessary to determine the radius, c,

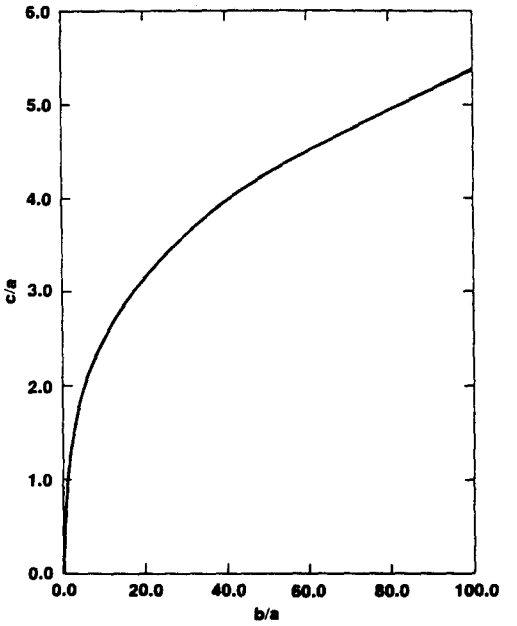

Fig. 1. Radius of the equivalent penny-shaped crack for a three-dimensional randomly oriented distribution of elliptical cracks.

of the "equivalent" penny-shaped crack. From eqns (25) and (26) it follows from equality of the respective crack density parameters, ε, that

$$c^3 = \frac{\pi\{ab^2\}}{2E(k)} \tag{40}$$

assuming equal number densities of elliptical and penny-shaped cracks. To illustrate the significance of the result in the context of micro-cracked ceramics, let us suppose that the family of ellipses has equal plan form (*not* merely similar). Thus

$$\left(\frac{c}{a}\right)^3 = \frac{\pi}{2}\frac{(b/a)^2}{E(k)}. \tag{41}$$

Figure 1 shows that the radius of the equivalent penny-shaped crack is particularly sensitive to aspect ratio. The slope of the curve shows that (c/a) is most sensitive to aspect ratio at $(b/a) = 1$. From a practical standpoint this means that knowledge of the number density of cracks, N, and one characteristic size (a) is not sufficient to calculate crack density and the resultant stiffness reduction. The sensitivity of stiffness reduction to aspect ratio is perhaps more clearly shown in Fig. 2 where stiffness reduction is plotted against crack density Na^3 for different values of b/a. As b/a is reduced from one, the stiffness reduction varies dramatically. Comparing results at $Na^3 = 0.2$ shows a stiffness reduction of $E/E_0 = 0.65$ for $b/a = 1$ as compared to $E/E_0 = 0.89$ for $b/a = 0.5$. *These observations show that knowledge of aspect ratio is essential in the determination of the correct family of equivalent penny-shaped cracks.* Despite the sensitivity of c to aspect ratio, we can still assert that it suffices to consider a randomly oriented distribution of penny-shaped cracks.

In order to avoid unnecessary complexity in the sequel, and in view of the preceding comments we do not consider elliptical cracks. Rather we focus on equivalent penny-shaped cracks. This decision is important in the next section because we can obtain analytic expressions for all but the final results.

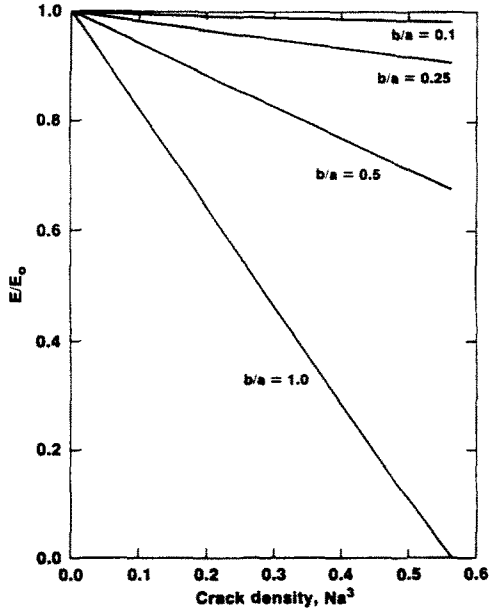

Fig. 2. Effect of aspect ratio on Young's modulus for a three-dimensional randomly oriented distribution of elliptical cracks ($\nu_0 = 0.25$).

5. ALIGNED PENNY-SHAPED CRACKS

In view of the comments at the end of Section 4, we here consider only a distribution of aligned penny-shaped micro-cracks. Hence, the cracked solid will be transversely isotropic with respect to the common normal to each crack, namely the x_3-axis. The self-consistent equation is from eqn (27)

$$M = M_0 + \tfrac{4}{3}\pi\varepsilon\Lambda^{\mathrm{p}} \tag{42}$$

where the components of the tensor Λ^{p} are given by eqns (13) and (14). In general, we note that there is no difficulty in allowing the uncracked material also to be transversely isotropic with respect to the x_3-axis. It is easily shown that the only components of the compliance tensor, M, which are changed by the introduction of cracks are M_{33}, M_{44} and M_{55}—but it is obvious that $M_{44} = M_{55}$. Thus, the equations of the self-consistent model are

$$M_{33} = M^0_{33} + \tfrac{4}{3}\pi\varepsilon\Lambda^{\mathrm{p}}_{33} \tag{43}$$

$$M_{44} = M^0_{44} + \tfrac{4}{3}\pi\varepsilon\Lambda^{\mathrm{p}}_{44} \tag{44}$$

where $\Lambda^{\mathrm{p}}_{33}$ and $\Lambda^{\mathrm{p}}_{44}$ are obtained from eqns (13) and (14). It is of interest to observe that this model has been explored in rather greater depth, but in a different context, by Laws and Dvorak[12].

At the present time, it is only prudent to consider solids which, when uncracked, are *isotropic*. This is particularly advantageous in the analysis of the model because it is not difficult to nondimensionalize the appropriate equations. Omitting details, we define

$$\omega = \left[\frac{E_0/E - \nu_0^2}{1-\nu_0^2}\right]^{1/2} \tag{45}$$

$$\rho = \left[\frac{2(G_0/G - \nu_0)}{1-\nu_0} + 2\left[\frac{E_0/E - \nu_0^2}{1-\nu_0^2}\right]^{1/2}\right]^{1/2} \tag{46}$$

it then follows that

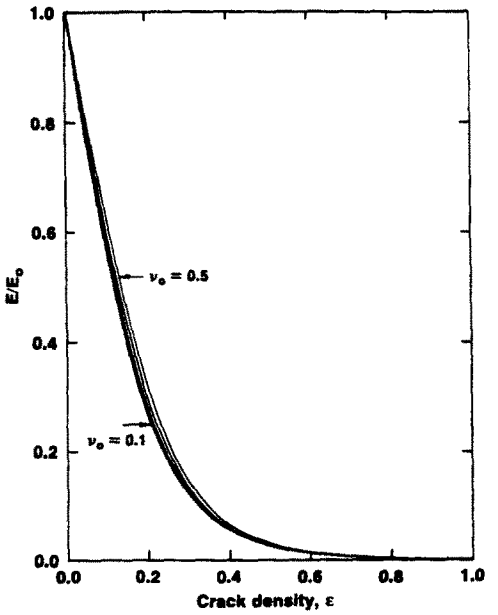

Fig. 3. Young's modulus for a distribution of aligned penny-shaped cracks.

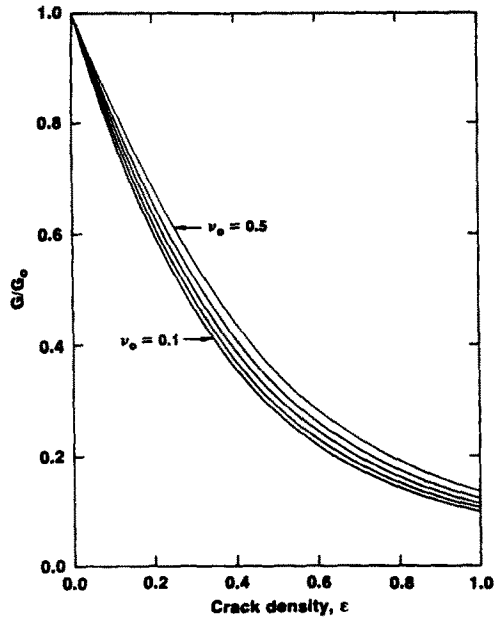

Fig. 4. Shear modulus for a distribution of aligned penny-shaped cracks.

$$\frac{E_0}{E} = 1 + \tfrac{8}{3}\varepsilon\rho\omega(1-\nu_0^2) \tag{47}$$

$$\frac{G_0}{G} = 1 + \frac{16}{3}\varepsilon\rho(1-\nu_0)\frac{(G_0/G)^{1/2}}{2(G_0/G)^{1/2}+\rho(1-\nu_0)}. \tag{48}$$

Equations (47) and (48) must be solved to give the loss in stiffness for a given crack density ε. If we interpret correctly, these equations agree with those obtained by Hoenig[8] by somewhat different methods.

The solutions of eqns (47) and (48) for E/E_0 and G/G_0 as a function of crack density ε are shown in Figs 3 and 4. The solution for E/E_0 shows little influence of initial Poisson's ratio ν_0. Because of the alignment of the cracks E tends to zero asymptotically as crack

density increases. The results for G/G_0 are similar although G does not decrease as fast as E for any crack density. Note that for E/E_0, the linear approximation would hold only over a small range of crack density. This is in contrast to the results for random pennies.

6. THREE-DIMENSIONALLY RANDOMLY ORIENTED SLIT CRACKS

We now consider a randomly oriented distribution of slit cracks. As in Section 2 we suppose that the length of the crack is l whereas its width is $2a \ll l$. In this case the self-consistent model is given by eqn (23)

$$M = M_0 + \pi\beta\{\Lambda^S\}. \tag{49}$$

In order to compare the stiffness loss for different micro-crack systems, it is essential to make use of a single crack density parameter. Thus we use the parameter ε defined in eqn (26)

$$\varepsilon = \frac{2N}{\pi}\left\{\frac{A^2}{P}\right\} = \frac{4}{\pi}\beta.$$

The self-consistent equation now reads

$$M = M_0 + \frac{\pi^2}{4}\varepsilon\{\Lambda^S\}. \tag{50}$$

As in the case of randomly oriented elliptical cracks we can calculate the orientation average of Λ^S using Kröner's[23] method. Again assuming that the uncracked solid is isotropic, we can, with minor changes, repeat the analysis of Section 4 to show that

$$\frac{E}{E_0} = 1 - \frac{\pi^2\varepsilon}{30}(1+\nu)(5-4\nu) \tag{51}$$

$$\frac{G}{G_0} = 1 - \frac{\pi^2\varepsilon}{60}(10-7\nu). \tag{52}$$

Also, we can express ν in terms of E and G and thus solve eqns (51) and (52) for E, G, ν, etc.

The loss of Young's modulus for randomly oriented slits and ellipses is shown in Fig.

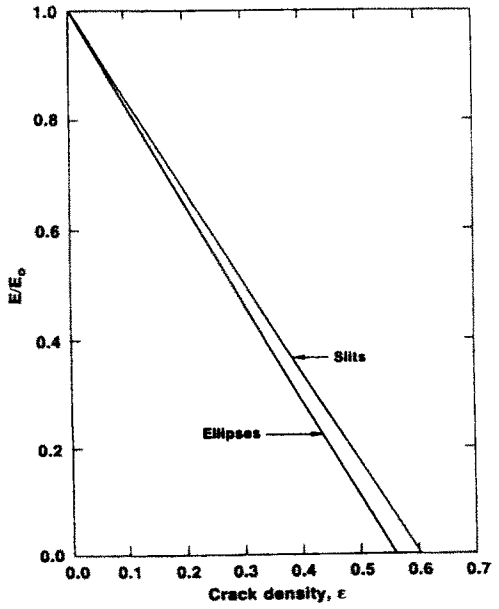

Fig. 5. Young's modulus for three-dimensional randomly oriented distributions of elliptical cracks and slit cracks.

5. We remark that interpretation of the proximity of these curves requires some care—as is emphasized in Ref. [2].

7. ALIGNED SLIT CRACKS

Consider next a distribution of fully aligned slit cracks in a solid. This particular problem has been analyzed in some detail by Laws *et al.*[10]. However, these authors were interested in composite laminates and so their analysis, while fully general, is not well suited to our present purpose. In any event, the self-consistent equations are here

$$M = M_0 + \pi^2 \frac{\varepsilon}{4} \Lambda^S. \tag{53}$$

For the crack alignment specified in expressions (5) the only non-vanishing components of Λ^S are given by eqns (7) and (8). It therefore follows that the only compliances which *change* because of cracks are M_{22}, M_{44}, and M_{66}. The first pair of these is given by the equations

$$M_{22} = M_{22}^0 + \frac{\pi^2 \varepsilon}{4} \Lambda_{22}^S \tag{54}$$

$$M_{66} = M_{66}^0 + \frac{\pi^2 \varepsilon}{4} \Lambda_{66}^S \tag{55}$$

whereas the shear compliance M_{44} is given by

$$M_{44} = M_{44}^0 + \frac{\pi^2 \varepsilon}{4} \Lambda_{44}^S. \tag{56}$$

We immediately specialize these results to the case in which the uncracked solid is isotropic, so that

$$M_{22}^0 = \frac{1}{E_0}, \qquad M_{44}^0 = M_{66}^0 = \frac{1}{G_0}.$$

Now let E be the Young's modulus of the cracked solid perpendicular to the crack faces

$$M_{22} = \frac{1}{E}. \tag{57}$$

Also let G_{II}, G_{III} be the shear moduli of the cracked solid associated with loading modes II and III, respectively

$$M_{66} = \frac{1}{G_{II}}, \qquad M_{44} = \frac{1}{G_{III}}. \tag{58}$$

A series of straightforward, but tedious, calculations shows that if we define

$$a = \left[2(1+\nu_0) \frac{G_0/G_{II} - \nu_0}{E_0/E - \nu_0^2} + 2\left[\frac{1-\nu_0^2}{E_0/E-\nu_0^2} \right]^{1/2} \right]^{1/2} \tag{59}$$

then

$$\frac{E_0}{E} = 1 + \frac{\pi^2 \varepsilon}{4} a \left[\frac{E_0}{E} - \nu_0^2 \right] \tag{60}$$

$$\frac{G_0}{G_{II}} = 1 + \frac{\pi^2 \varepsilon}{8} a \left[\frac{E_0}{E} - \nu_0^2 \right]^{1/2} \left[\frac{1-\nu_0}{1+\nu_0} \right]^{1/2}. \tag{61}$$

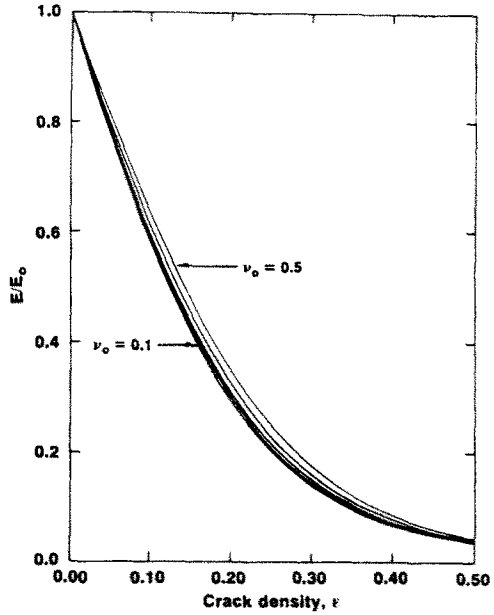

Fig. 6. Young's modulus for a distribution of aligned slit cracks in an isotropic solid.

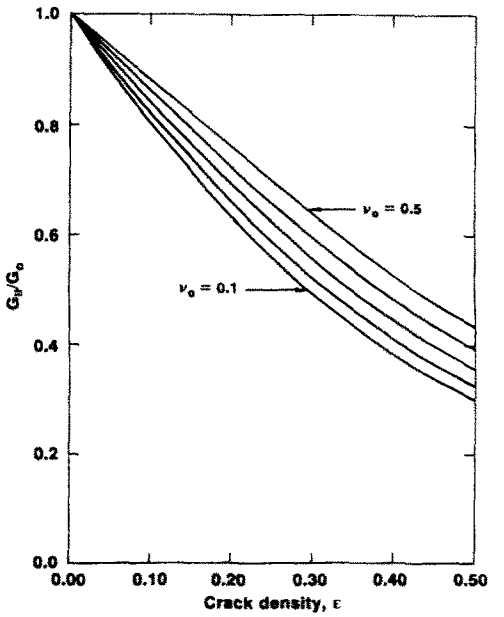

Fig. 7. Mode II shear modulus for a distribution of aligned slit cracks in an isotropic solid.

These equations serve to evaluate E/E_0 and G_{II}/G_0 for a given crack density ε. In addition we can show that G_{III}/G_0 is given explicitly as

$$G_{III}/G_0 = \frac{1}{64}[-\pi^2\varepsilon+(\pi^4\varepsilon^2+64)^{1/2}]^2. \tag{62}$$

The solutions to eqns (60) and (61) for E/E_0 and G_{II}/G_0 are expressed as a function of initial Poisson's ratio in Figs 6 and 7. These results are similar to those for aligned pennies (Figs 3 and 4) in that both E/E_0 and G_{II}/G_0 approach zero asymptotically as crack density increases with E/E_0 decreasing faster than G_{II}/G_0. The result for G_{III}/G_0 (Fig. 8) is independent of initial Poisson's ratio and also approaches zero asymptotically.

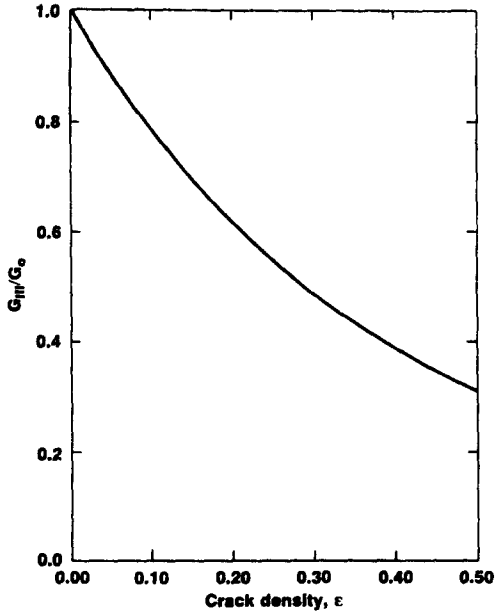

Fig. 8. Mode III shear modulus for a distribution of aligned slit cracks in an isotropic solid.

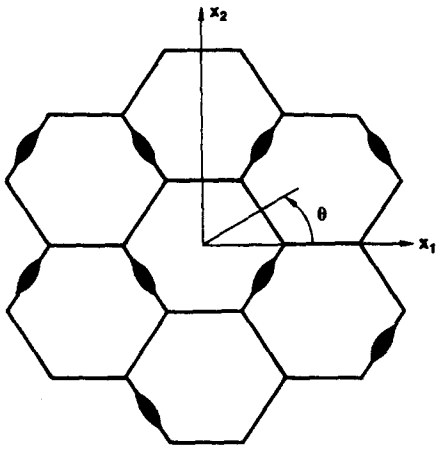

Fig. 9. Hexagonal array with cracks at interfaces: equal crack densities on planes $\theta = 0, \pm\pi/3$.

8. TWO-DIMENSIONALLY ORIENTED SLIT CRACKS

In this section we examine the stiffness loss due to two distributions of two-dimensionally oriented slit cracks. In the first place we consider a family of slit cracks whose normals are arbitrarily oriented in the x_1–x_2 plane—i.e. the axis of the crack lies along the x_3-axis. Second we consider a hexagonal close-packed polycrystalline array with cracks on various facets as suggested by Fu and Evans[6], see Fig. 9. For simplicity we assume equal crack number density on the three families of parallel faces. Both models are susceptible of refinement and generalization. At the present time the two models furnish an additional potential geometry for microstructures in cracked ceramics. It is interesting to declare in advance that the assumed geometry of cracks in an otherwise isotropic solid guarantees transverse isotropy and that both geometries give rise to the *same* stiffness reduction. In addition we are able to obtain explicit formulae—which is significant from the point of view of applications.

It is clear that the cracked solid will be transversely isotropic with respect to the x_3-axis. Thus, the compliance tensor of the cracked solid is of the form of eqns (3) and (4) with respect to any set of axes $0x'_1x'_2x_3$ which are obtained from $0x_1x_2x_3$ by rotation through an angle θ. In addition, transverse isotropy guarantees that the components of the Λ^S tensor with respect to $0x'_1x'_2x_3$ are precisely the same as those with respect to $0x_1x_2x_3$.

A concise derivation of the models can be given by using the device suggested by Bristow[24]. In order to compute the average interaction energy $\{\mathscr{E}\}$ we have so far averaged over the relevant orientations of the cracks under fixed loads $\bar{\sigma}$. However, as noted by Bristow[24] we can equally well leave the cracks fixed and average over all orientations of the applied load. Thus, we return to eqn (19) which gives us the required expression for the interaction energy due to a single slit crack located at

$$-a \leqslant x_1 \leqslant a, \qquad x_2 = 0, \qquad |x_3| < l \tag{63}$$

under applied stress $\bar{\sigma}$

$$\mathscr{E} = \tfrac{1}{2}\pi a^2 l \bar{\sigma} \cdot \Lambda^S \bar{\sigma}. \tag{64}$$

Next we rotate the applied stress field $\bar{\sigma}$ through an angle θ to give the field $\bar{\sigma}'(\theta)$ which is, of course, determined from the usual tensor transformation. The only components of interest are

$$\begin{aligned}
\bar{\sigma}'_{22}(\theta) &= \bar{\sigma}_{11} \sin^2 \theta - 2\bar{\sigma}_{12} \sin \theta \cos \theta + \bar{\sigma}_{22} \cos^2 \theta, \\
\bar{\sigma}'_{23}(\theta) &= -\bar{\sigma}_{13} \sin \theta + \bar{\sigma}_{23} \cos \theta, \\
\bar{\sigma}'_{21}(\theta) &= (\bar{\sigma}_{22} - \bar{\sigma}_{11}) \sin \theta \cos \theta + \bar{\sigma}_{12}(\cos^2 \theta - \sin^2 \theta).
\end{aligned} \tag{65}$$

Remembering that the components of Λ^S are not changed by rotation of the axes through an angle θ, it follows that the interaction energy for the crack, given by (63), under loading $\bar{\sigma}'(\theta)$ is

$$\mathscr{E}(\theta) = \tfrac{1}{2}\pi a^2 l \bar{\sigma}'(\theta) \cdot \Lambda^S \bar{\sigma}'(\theta). \tag{66}$$

Consider first the case of two-dimensionally randomly oriented slits. If we again assume that crack size and orientation are not correlated, we can show that

$$\begin{aligned}
\{\mathscr{E}\} &= \frac{\pi \varepsilon}{8N} \int_0^{\pi} \bar{\sigma}'(\theta) \cdot \Lambda \bar{\sigma}'(\theta) \, \mathrm{d}\theta \\
&= \frac{\pi^2}{8N} \varepsilon \bar{\sigma} \cdot \{\Lambda\} \bar{\sigma}
\end{aligned} \tag{67}$$

where the non-vanishing components of $\{\Lambda\}$ are given by

$$\begin{aligned}
\{\Lambda\}_{11} &= \{\Lambda\}_{22} = \tfrac{1}{8}(3\Lambda_{22} + \Lambda_{66}), \\
\{\Lambda\}_{12} &= \tfrac{1}{8}(\Lambda_{22} - \Lambda_{66}), \\
\{\Lambda\}_{44} &= \{\Lambda\}_{55} = \tfrac{1}{2}\Lambda_{44}, \\
\{\Lambda\}_{66} &= \tfrac{1}{2}(\Lambda_{22} + \Lambda_{66}).
\end{aligned} \tag{68}$$

We note that

$$\{\Lambda\}_{11} - \{\Lambda\}_{12} = \tfrac{1}{2}\{\Lambda\}_{66}$$

as is required for transverse isotropy with respect to $0x_3$.

Next consider the case of the hexagonally packed array. Here each family of parallel faces contains one third of the total number of cracks. Also to ensure transverse isotropy we again need to assume that crack size is not correlated to crack orientation. In this case it is clear that

$$\{\mathscr{E}\} = \tfrac{1}{3}[\mathscr{E}(0)+\mathscr{E}(\pi/3)+\mathscr{E}(-\pi/3)].$$

It is significant that the result of this simple averaging procedure is precisely the same as the result for two-dimensionally randomly oriented slits given in eqns (67) and (68). Thus the self-consistent model in either case is

$$M = M_0 + \frac{\varepsilon}{4}\pi^2\{\Lambda^S\} \tag{69}$$

where the components of $\{\Lambda\}^S$ are given in eqns (68).

Finally we exhibit the explicit form of the equations where the uncracked solid is isotropic with Young's modulus E_0, Poisson's ratio ν_0 and shear modulus G_0. Since the cracked material is transversely isotropic with respect to $0x_3$, we denote the axial shear modulus by G_A, the transverse shear modulus by G_T and the transverse Young's modulus by E_T. In terms of the compliances

$$\begin{aligned} M_{11} &= M_{22} = \frac{1}{E_T}, \\ M_{44} &= \frac{1}{G_A}, \qquad M_{66} = \frac{1}{G_T}. \end{aligned} \tag{70}$$

It is evident physically, and demonstrable mathematically from eqn (69), that the only compliances which are changed by the micro-crack distribution are M_{11}, M_{12}, $M_{44} = M_{55}$ and M_{66}. But since

$$M_{66} = 2(M_{11} - M_{12})$$

it suffices to concentrate on M_{11}, M_{44} and M_{66}. From eqn (8) we note that transverse isotropy implies that $\alpha_1 = \alpha_2 = 1$, so from eqns (7) we have

$$\begin{aligned} \Lambda^S_{22} = \Lambda^S_{66} &= 2\frac{M_{11}M_{33} - M_{13}^2}{M_{33}} \\ \Lambda^S_{44} &= M_{44}. \end{aligned}$$

But, the simplification afforded by isotropy of the uncracked solid shows that

$$\begin{aligned} \Lambda^S_{22} = \Lambda^S_{66} &= 2\left(\frac{1}{E_T} - \frac{\nu_0^2}{E_0}\right) \\ \Lambda^S_{44} &= \frac{1}{G_A}. \end{aligned}$$

Thus from eqns (68)

$$\begin{aligned} \{\Lambda^S\}_{11} &= \frac{1}{E_T} - \frac{\nu_0^2}{E_0}, \\ \{\Lambda^S\}_{44} &= \frac{1}{2G_A}, \\ \{\Lambda^S\}_{66} &= 2\left(\frac{1}{E_T} - \frac{\nu_0^2}{E_0}\right). \end{aligned} \tag{71}$$

We may now substitute eqns (71) into eqn (69) to obtain the final results

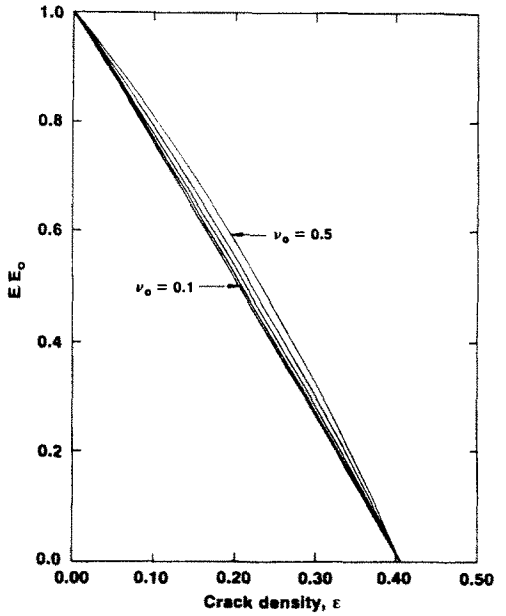

Fig. 10. Transverse Young's modulus for distributions of two-dimensionally oriented slit cracks in isotropic materials.

$$\frac{E_T}{E_0} = \frac{4-\pi^2\varepsilon}{4-\pi^2\varepsilon\nu_0^2} \tag{72}$$

$$\frac{G_T}{G_0} = \frac{4-\pi^2\varepsilon}{4-\pi^2\varepsilon\nu_0} \tag{73}$$

$$\frac{G_A}{G_0} = 1 - \frac{\pi^2\varepsilon}{8}. \tag{74}$$

It is quite remarkable that the two geometries considered above give rise to the explicit formulae (72)–(74) for the loss of stiffness due to micro-cracks. The results for E/E_0 for varying values of initial Poisson's ratio are shown in Fig. 10. As in the case of random pennies and slits, stiffness is reduced to zero at a particular value of crack density. From eqns (72) and (73) we see that both E_T and G_T vanish when $\varepsilon = 4/\pi^2$. Although G_A, as given in eqn (74), does not vanish until the crack density $\varepsilon = 8/\pi^2$, it is clear that $\varepsilon = 4/\pi^2$ is the maximum permissible value of the crack density, see Fig. 11. However, it is unlikely that the self-consistent method would apply at such extremes. The result for the transverse shear modulus G_T/G_0 (Fig. 12) is similar to results for random pennies and slits. Poisson's ratio ν_{12} changes for this crack system and is given by

$$\nu_{12} = \frac{(1+\nu_0)(E_T/E_0)}{G_T/G_0} - 1.$$

The variation of ν_{12} with crack density is plotted in Fig. 13 and of course depends on the initial Poisson's ratio.

9. COMPARISON OF CRACK SYSTEMS

Despite our use of a universal crack density parameter

$$\varepsilon = \frac{2N}{\pi}\left\{\frac{A^2}{p}\right\} \tag{75}$$

comparison of the effect of different crack systems is not easy. Even for materials which

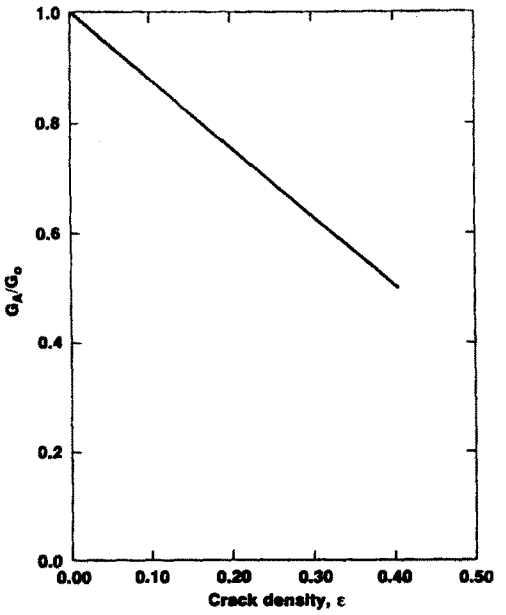

Fig. 11. Axial shear modulus for distributions of two-dimensionally oriented slit cracks in isotropic materials.

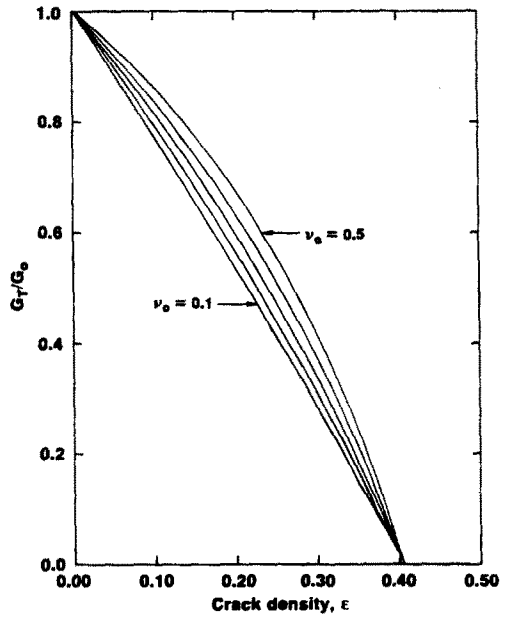

Fig. 12. Transverse shear modulus for distributions of two-dimensionally oriented slit cracks in isotropic materials.

are initially isotropic, the most obvious problem is that micro-crack geometry can induce macroscopic anisotropy. Indeed, of the various geometries considered here, only randomly oriented slits or ellipses yield overall isotropic response. On the other hand, two-dimensional randomly oriented slit cracks (or hexagonal close packed aggregates) lead to overall transverse isotropy as do aligned penny-shaped cracks. In addition, aligned slits lead to orthotropic materials.

At this stage it is essential to recall one of our basic premises that all cracks are *open* under the considered loading. We emphasize that the results obtained in this report only hold for the case of *open* cracks. In fact it is not difficult to see that under certain types of loading this will *not* be the case. Consider, for example, pure shear of the two-dimensionally random distribution of slit cracks. Here it is clear that half of the cracks will be open

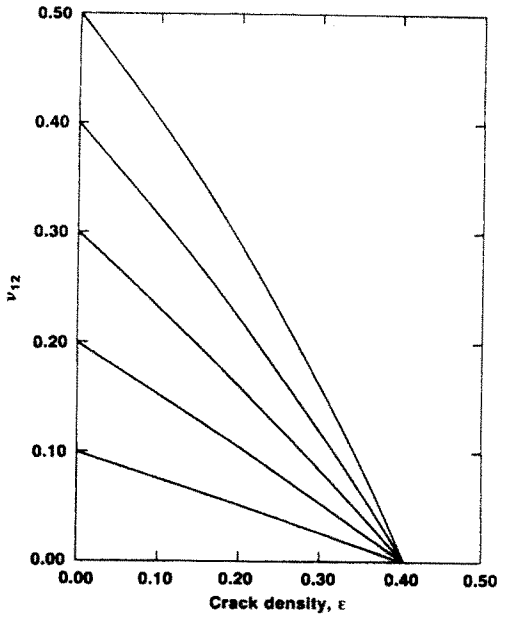

Fig. 13. Poisson's ratio ν_{12} for distributions of two-dimensionally randomly oriented slit cracks in isotropic materials.

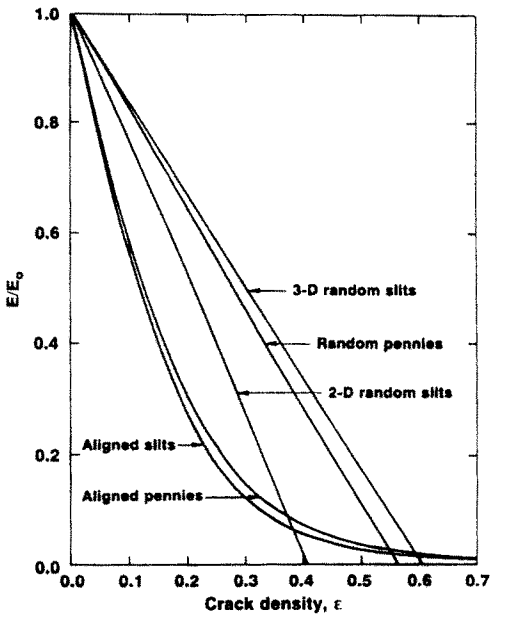

Fig. 14. Composition of stiffness reduction in isotropic materials for different crack systems ($\nu_0 = 0.25$).

whereas the other half will remain closed under the stated loading. This problem, and other related issues, will be discussed in a future paper.

Returning now to a quantitative assessment of the effect of various micro-crack geometries, let us consider a family of cracked materials with *common crack density* ε. In order to illustrate the effect of geometry on the loss of stiffness of the solid, we consider the worst possible scenario. Thus for aligned slits or pennies we need to evaluate Young's modulus for extension normal to the slits or pennies. For two-dimensional randomly oriented slits—or slits on the faces of a hexagonal close packed aggregate—we evaluate Young's modulus in any direction in the basal plane. Of course for three-dimensional randomly oriented slits or ellipses, Young's modulus is independent of direction. The results are given in Fig. 14. We note that the reductions in Young's modulus for three-dimensional randomly oriented slits or ellipses are quite comparable, as are the reductions for aligned slits and pennies.

Choice of ε as the appropriate density measure, see eqn (75), demands that care is essential if any general inferences are to be drawn from Fig. 14. Clearly the problem is that ε is the product of crack number density and a geometrical factor. Perhaps it is easiest to illustrate the point with reference to *dilute* distributions of cracks—and as will now be shown, it is likely that the dilute limit will be completely satisfactory in many applications. In the case of aligned slits the Young's modulus normal to the slits is, from eqn (60)

$$\frac{E}{E_0} = 1 - \frac{\pi^2}{2}(1-\nu_0^2)\varepsilon \tag{76}$$

whereas for aligned pennies, from eqn (47)

$$\frac{E}{E_0} = 1 - \frac{16}{3}(1-\nu_0^2)\varepsilon. \tag{77}$$

Also, for two-dimensional randomly oriented slits we have, from eqn (72)

$$\frac{E}{E_0} = 1 - \frac{\pi^2}{4}(1-\nu_0^2)\varepsilon. \tag{78}$$

Finally, for three-dimensional randomly oriented slits we have, from (51)

$$\frac{E}{E_0} = 1 - \frac{\pi^2}{30}(1+\nu_0)(5-4\nu_0)\varepsilon \tag{79}$$

and for randomly oriented pennies, from eqn (38)

$$\frac{E}{E_0} = 1 - \frac{16(1-\nu_0^2)(10-3\nu_0)}{45(2-\nu_0)}\varepsilon. \tag{80}$$

Thus when $\nu_0 = 0.25$, as in Fig. 14, we can easily compute the residual stiffness for the various geometries. By way of illustration take $\varepsilon = 0.05$, then the residual Young's modulus is as follows:

three-dimensional randomly oriented slits	92%
three-dimensional randomly oriented pennies	91%
two-dimensional randomly oriented slits	88%
aligned slits	77%
aligned pennies	75%.

Thus, as noted earlier, *the dilute approximation will be entirely adequate for most applications.*

From eqns (76), (78) and (79) it is easy to compare the relative *numbers* of similar slit cracks with different orientations which would be needed to produce the same loss of Young's modulus. Thus, suppose that the same loss of stiffness is produced by N_a aligned slits, N_2 two-dimensional randomly oriented slits or N_3 three-dimensional randomly oriented slits. Then

$$N_a = \tfrac{1}{2}N_2 = \frac{5-4\nu_0}{15(1-\nu_0)}N_3.$$

Again suppose that n_a aligned pennies produce the same loss of stiffness as n_3 randomly oriented pennies, then from eqns (77) and (80)

$$n_a = \frac{10 - 3\nu_0}{15(2 - \nu_0)} n_3.$$

It is more difficult to compare the numbers of aligned slits or pennies which would produce the same loss of stiffness. The problem is that one needs to have some information about the respective geometries. Until some experimental evidence is available it is of little value to compare hypothetical cases. In any case, the required results are easily obtained from eqns (76) to (80).

In conclusion we observe that knowledge of crack number density, orientation distribution and crack geometry are essential in order to predict the loss in stiffness of a cracked solid.

Acknowledgements—The work of one of us (N. Laws) was supported in part by the Aluminum Company of America. We thank Mr R. L. Rolf and Dr J. L. Teply for many helpful discussions.

REFERENCES

1. E. D. Case, The effect of microcracking upon the Poisson's ratio for brittle materials. *J. Mater. Sci.* **19,** 3702–3712 (1984).
2. B. Budiansky and R. J. O'Connell, Elastic moduli of a cracked solid. *Int. J. Solids Structures* **12,** 81–97 (1976).
3. A. G. Evans, Microfracture from thermal expansion anisotropy—I. Single phase systems. *Acta Metall.* **26,** 1845 (1978).
4. A. G. Evans and K. T. Faber, Crack growth resistance of microcracking brittle materials. *J. Am. Ceram. Soc.* **67,** 255–260 (1983).
5. Y. Fu and A. G. Evans, Microcrack zone formation in single phase polycrystals. *Acta Metall.* **30,** 1619–1625 (1982).
6. Y. Fu and A. G. Evans, Some effects of microcracks on the mechanical properties of brittle solids—I. Stress, strain relations. *Acta Metall.* **33,** 1515–1523 (1985).
7. Y. Fu and A. G. Evans, Some effects of microcracks on the mechanical properties of brittle solids—II. Microcrack toughening. *Acta Metall.* **33,** 1525–1531 (1985).
8. A. Hoenig, Elastic moduli of a non-randomly cracked body. *Int. J. Solids Structures* **15,** 137–154 (1979).
9. T. Gottesman, Z. Hashin and M. A. Brull, Effective elastic moduli of cracked fiber composites. In *Advances in Composite Materials* (Edited by A. R. Bunsell, A. Martrenchar, D. Menkes, C. Bathias and G. Verchery), pp. 749–758. Pergamon Press, Oxford (1980).
10. N. Laws, G. J. Dvorak and M. Hejazi, Stiffness changes in unidirectional composites caused by crack systems. *Mech. Mater.* **2,** 123–137 (1983).
11. H. Horii and S. Nemat-Nasser, Overall moduli of solids with microcracks: load induced anisotropy. *J. Mech. Phys. Solids* **31,** 155–171 (1983).
12. N. Laws and G. J. Dvorak, The effect of fiber breaks and aligned penny-shaped cracks on the stiffness and energy release rates in unidirectional composites. *Int. J. Solids Structures* **23,** 1269–1283 (1987).
13. R. Hill, Elastic properties of reinforced solids: some theoretical principles. *J. Mech. Phys. Solids* **11,** 357–372 (1963).
14. A. N. Stroh, Dislocations and cracks in anisotropic elasticity. *Phil. Mag.* **3,** 625–646 (1958).
15. S. G. Lekhnitskii, *Anisotropic Plates*. Gordon and Breach, New York (1968).
16. G. C. Sih, P. C. Paris and G. R. Irwin, On cracks in rectilinearly anisotropic bodies. *Int. J. Fracture Mech.* **1,** 189–203 (1965).
17. N. Laws, A note on interaction energies associated with cracks in anisotropic media. *Phil. Mag.* **36,** 367–372 (1977).
18. R. T. Shield, Notes on problems in hexagonal aeolotropic materials. *Proc. Camb. Phil. Soc.* **47,** 401–409 (1951).
19. W. T. Chen, Some aspects of a flat elliptical crack under shear stress. *J. Math. Phys.* **45,** 213–223 (1966).
20. T. Mura, *Micromechanics of Defects in Solids*. Martinus Nijhoff, The Hague (1982).
21. N. Laws, A note on penny-shaped cracks in transversely isotropic materials. *Mech. Mater.* **4,** 209–212 (1985).
22. J. D. Eshelby, Elastic inclusions and inhomogeneities. In *Progress in Solid Mechanics* (Edited by I. N. Sneddon and R. Hill), Vol. 2. North Holland, Amsterdam (1957).
23. E. Kröner, Berechnung der elastichen Konstanten des Vielkristalls aus den Konstanten des Einkristalls. *Z. Phys.* **151,** 504–518 (1958).
24. J. R. Bristow, Microcracks, and the static and dynamic elastic constants of annealed and heavily cold-worked metals. *Br. J. Appl. Phys.* **11,** 81–85 (1960).